CAVEAT EMPTOR: SPURIOUS SPIN VECTORS FROM INCORRECT SIDEREAL PERIODS

Stephen M. Slivan
Massachusetts Institute of Technology,
Dept. of Earth, Atmospheric, and Planetary Sciences
77 Mass. Ave. Rm. 54-410, Cambridge, MA 02139
slivan@mit.edu

(Received: 2021 June 16, Revised: 2021 July 28)

Spin vector and shape solutions are among the most sophisticated and nuanced analyses that might be undertaken by lightcurve observers who compile measurements from multiple apparitions. Unambiguously determining the correct sidereal period before attempting convex inversion is key, because an incorrect period leads naturally to a spurious spin vector solution. A specific case study for (1443) Ruppina is examined here, with advice on how to recognize an incorrect sidereal period and avoid proceeding with a convex inversion analysis that will be spurious.

Introduction

Convex inversion is a powerful tool for modeling asteroid shapes from lightcurves, but care must be taken to use it correctly. Its design as a nonlinear iterative algorithm (Kaasalainen et al., 2001) requires that initial values be supplied for several parameters including the sidereal rotation period, which the algorithm will be unable to correct if the value is systematically wrong. Instead, it will use the many degrees of freedom at its disposal to do its powerful best and deliver a solution based on the faulty input values, yielding results which might appear to be reasonable despite in fact being spurious. Similarly, quietly wrong outcomes are possible if the available epoch information is not sufficient to distinguish the correct sidereal period. A series of articles in the *Minor Planet Bulletin* (Slivan, 2012; 2013; 2014) discusses the issues related to counting rotations across a lightcurve data set spanning multiple apparitions, and presents information to help manage ambiguity and avoid incorrect determinations of sidereal periods.

A published analysis for asteroid (1443) Ruppina by Stephens and Warner (2020), hereafter "S&W20," provides an instructive case study. The authors observed lightcurves of Ruppina during its 2020 apparition, and combined it with lightcurves from one prior apparition (Stephens, 2018) plus "sparse data" to report a sidereal rotation period result of 5.87929 h. They also reported a corresponding spin vector solution obtained using convex inversion, with one retrograde pole at (120°; –15°) and inconsistent locations given for the symmetric retrograde pole—the text on p. 276 says (295°;–22°) but the Fig. 4 on p. 277 says (300°;–15°). (Note that in the article, figure numbers 1 through 6 are each assigned to two different figures.).

The information in the S&W20 Fig. 1 on p. 277 and accompanying text, suggests that the initial value for the sidereal period was selected based on a statistical approach of identifying a global minimum in a noise spectrum. However, the model used as the basis for the calculations is neither identified nor explained for the reader, and despite including only two published lightcurves, no basis is discussed for confidence that the approach identified the correct sidereal period and merited subsequent spin vector determination. There are other indications in the article that warrant caution, mainly that the graphs of selected lightcurve fits presented as the S&W20 Fig. 5/6 on p. 277 show that, contrary to the caption, the model lightcurves are not "very close on all occasions"—both graphs show systematic mismatches in the shapes of the fitted model lightcurve minima, near phase 0.6 in 2017 and near phase 0.2 in 2020, that appear to be corroborated by the composited lightcurves' graphs in their original publications (Stephens, 2018, p. 51; Stephens and Warner, 2020, p. 276). Also, with regard to the identification of a preferred solution from the symmetric pair of poles, Earth-based lightcurves cannot resolve the ambiguity for Ruppina because of its low orbit inclination of only 2 degrees; thus, a solution that statistically significantly favors one region over the other would be suspect.

Considering especially the limited data upon which the solution is based, a first place to check for a problem is the sidereal period. Slivan (2013) has already detailed for lightcurve observers how to calculate a comprehensive set of sidereal period ranges that are consistent with a set of lightcurve epochs, a calculation which will be used here to test whether the sidereal period solution is consistent with epochs from the four apparitions from which lightcurves have previously been published. The first step is to identify appropriate upper and lower bounds on the sidereal rotation period informed by the best constraint on the synodic rotation period, as illustrated here for Ruppina.

Synodic constraints on sidereal period

For Ruppina the synodic period is very secure as there had already been published four independent determinations, all of which agree (Neugent and Slivan, 2008; Arredondo et al., 2014; Stephens, 2018; Stephens and Warner, 2020). The statistically optimal combination of the measurements is the mean of the individual values weighted by the inverse squares of their errors, yielding 5.8800 ± 0.0006 h. (Note that there is a typographic error in Stephens (2018), p. 51, col. 2, line 3, where the period should read "5.88 h".) However, a subtlety arises from the individual periods' errors having been rounded to a single significant digit—each of the 0.001-h errors could represent unrounded values of up to 0.0015 h, which would underreport the magnitude of the error by up to one-third of its value. In the context of particular priority to not underestimate the allowed range of periods, the possible effect of such rounding is accounted for here by increasing the error of the weighted mean proportionally to ± 0.0009 h.

This one-sigma error corresponds to a confidence interval of about 68%. Adopting 2.5σ to use a more inclusive confidence interval of about 99% as the estimated bounds on the sidereal period yields the range 5.8777 to 5.8823 h.

A remaining consideration is the systematic difference between the sidereal period and the synodic period. For a main-belt object such as Ruppina this difference is too small to distinguish during a single apparition, but for completeness let us consider here what the effect of changing viewing aspect on the measured synodic period actually is. Ephemeris calculations using JPL HORIZONS indicate that for Ruppina the maximum rate of change in phase angle bisector (PAB) longitude is about 0.00088°/h which occurs near oppositions in February or March. This rate corresponds to a maximum possible apparent period change of 0.000084 h per rotation, which can be accounted for here by expanding the bounded interval by only another 0.0001 h at both ends. Thus, the corresponding constraint on the sidereal period for Ruppina, based on the ~99% confidence interval, is 5.8776 to 5.8824 h.

The span of the S&W20 Fig. 1 graph on p. 277 is more than 50 times wider than the synodic constraint, which compresses the bounded range into just over a millimeter, and renders unreadable the only part of the graph that is pertinent to determining the sidereal period. A constructive suggestion for an informative presentation instead would be to illustrate in detail the behavior of the chi-square values within the bounded range, accompanied by context information documenting the model used to calculate the values plotted on the graph.

Published data rule out the reported sidereal period

With the synodic constraint as an input, the "sieve algorithm" of Slivan (2013) is used here to identify the ranges of sidereal periods allowed by the epochs of the already-published lightcurves of Ruppina (Table I). The estimated epoch measurement errors used are 15 min, which is 1.5× the maximum observed asymmetry of the timing of the extrema in the composite lightcurves. A graphical presentation of the results (Fig. 1) shows more than one allowed range for the sidereal period, indicating that these epochs are not sufficient to unambiguously count rotations. Nevertheless, they are sufficient to show that the reported period solution falls outside all of the allowed ranges, thus ruling it out as not consistent with the published lightcurves.

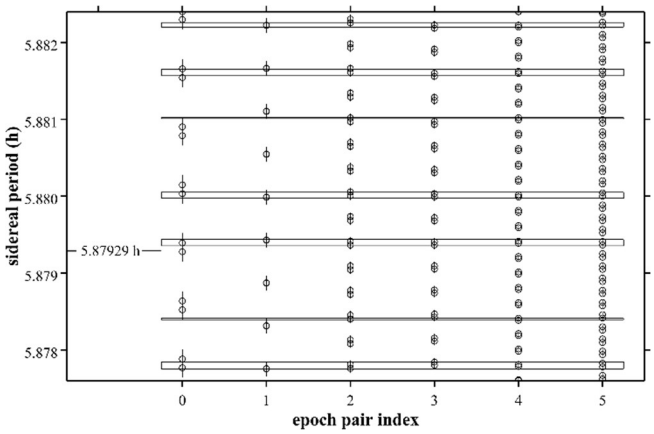

Figure 1: Ranges of possible sidereal rotation periods of (1443) Ruppina allowed by the epochs in Table I, within the synodic constraint 5.8776 to 5.8824 h. Each horizontal coordinate index corresponds to the time interval between a pair of epochs as detailed in Table II, ordered with longer intervals to the right. Open circles and vertical bars represent sidereal periods and period ranges, respectively, calculated from every possible number of rotations that could elapse during the interval. Thin horizontal rectangles identify the ranges of periods that are allowed by all six time intervals. Also marked is the period solution of S&W20, which is not within any of the allowed ranges.

Comparing the sidereal period and poles with a solution based on sufficient data

A key implication of the nonlinear nature of convex inversion is that a small systematic error in the sidereal period can easily produce a huge systematic error in the pole. In the context of the present case study, it would be instructive to be able to also demonstrate here how much of a difference using this incorrect sidereal period actually made in the pole location result reported.

As shown above, epochs from the previously published lightcurves available for Ruppina do not resolve the correct sidereal period for such a demonstration. However, additional lightcurves being reported in a companion paper (Slivan, 2021; this issue) make the needed solution possible—the expanded data set satisfies the criteria of Slivan (2012; 2013; 2014) to unambiguously count rotations and determine a secure sidereal period suitable for spin vector solution, specifically avoiding relying on a statistical noise spectrum. As is fully reported with the additional lightcurves, the analysis determines a sidereal period of 5.87941 h and a symmetric pair of prograde poles near (160°;+79°) and (358°;+79°). That solution based on data from five apparitions predates lightcurves from the 2020 apparition but is consistent with those data; including them in the analysis as a sixth apparition (Fig. 2) leaves the sidereal period unchanged and nudges the pole location by less than one degree of arc.

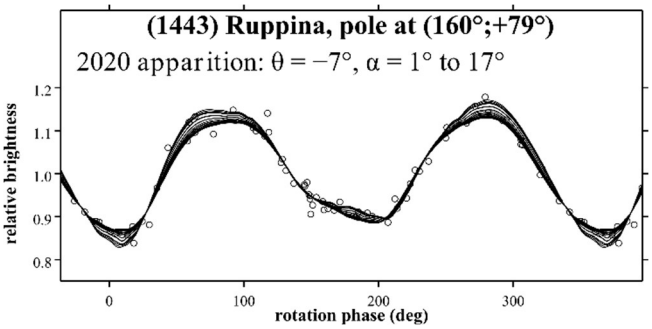

Figure 2: Lightcurve model fits to the same ATLAS-MLO data from 2020 identified in the caption for Table I, as brightness vs. sidereal rotation phase for the P_1 solution of (1443) Ruppina reported by Slivan (2021; this issue), formatted identically to Fig. 4 in that same paper for easy comparison. Open circles represent observed brightnesses; solid curves represent the model. Changes in the lightcurve shape during the course of the observations appear as non-overlapping model curves. θ is the sub-PAB latitude and α is the included range of solar phase angles.

Fig. 2 also permits a visual consistency check of relative amplitudes expected for the pole positions from the two analyses, as a function of the asterocentric latitudes θ of the phase angle bisectors ("sub-PAB latitudes"). For the pole at (160°;+79°) the viewing geometry remains always close to equatorial, predicting that the lightcurves will all exhibit similar amplitudes as has been observed (Slivan, 2021, Fig. 4; this issue). In contrast, for a pole solution at (120°;–15°) the viewing aspect in 2020 at θ = +13° would be similar to equatorial, but the aspect in 2014 at θ = –60° would be more than 45 degrees farther from equatorial and closer to pole-on, predicting a significantly smaller relative amplitude in 2014 that is not consistent with the observations.

Note that while the sidereal periods of the two analyses differ by only 0.00012 h, that small error in the period produced a pole location error of more than 90 degrees of arc; in other words, the spurious pole solutions are not even approximately correct. It demonstrates the importance of understanding that a wrong sidereal period is a systematic error rather than a statistical error, and also shows clearly how insidiously wrong a spurious solution can be as it is effectively a random result.

Conclusion

When using convex inversion to model spins and shapes from lightcurves, supplying the correct sidereal period is required in order to have confidence in the results, even to qualify them as 'preliminary' or as 'possible.' The need for sufficient epoch information and proper attention to its analysis remains unchanged whether using dense published lightcurves or sparse data from surveys:

Precept 1: Don't underestimate the effort—the sidereal period is a full-fledged science result on its own requiring and deserving due respect.

Precept 2: Don't underestimate the importance—markedly wrong spin vectors result from even slightly wrong sidereal periods.

UT epoch	PAB λ,β(°)
2007 Nov 07 0.99 h	68.6 −2.2
2014 Feb 23 1.08 h	146.8 −1.1
2017 Sep 05 0.68 h	56.3 −1.6
2020 Apr 16 1.75 h	222.7 +1.7

Table I: Summary of (1443) Ruppina lightcurve epochs, in each case locating a maximum from the second harmonic of a Fourier series model that was fit to lightcurves. The 2007 and 2014 epochs are measured from the observations reported by Neugent and Slivan (2007) and by Arredondo et al. (2014), respectively. The 2017 epoch is measured from the observations reported by Slivan (2021; this issue) composited to the same date as the lightcurves of Stephens (2018, p. 51). The 2020 epoch is measured from ATLAS-MLO survey (Tonry et al., 2018) *o*-band photometry recorded between the stationary points of the 2020 apparition, retrieved from the MPC Orbits/Observations Database and composited to the same date as the lightcurves of Stephens and Warner (2020, p. 276). λ,β are J2000 ecliptic longitude and latitude of the phase angle bisector (PAB).

Epoch pair index	Interval (d)	Interval (app.)	Epochs source apparitions
0	954.0	2	2017, 2020
1	1290.0	3	2014, 2017
2	2244.0	5	2014, 2020
3	2300.0	5	2007, 2014
4	3590.0	8	2007, 2017
5	4544.0	10	2007, 2020

Table II: Time intervals between the epochs given in Table I, used to identify the ranges of sidereal periods allowed by the already-published lightcurves of (1443) Ruppina. Columns are: the epoch pair index label used in Fig. 1, the interval length rounded to 0.1 d, the corresponding integer count of elapsed apparitions, and identification of the apparitions from which the defining epochs were measured.

Acknowledgements

I thank Dr. Richard Binzel for suggestions that improved this paper. This work has made use of data and services provided by the International Astronomical Union's Minor Planet Center; specifically, the brightnesses accompanying astrometry from the Asteroid Terrestrial-impact Last Alert System (ATLAS) survey observing program.

References

Arredondo, A.; Hartt, A.; Yazdi, S.K. (2014). "Rotation Periods and *R* Magnitudes of Three Koronis Family Members." *Minor Planet Bull.* **41**, 252-254.

Kaasalainen, M.; Torppa, J.; Muinonen, K. (2001). "Optimization methods for asteroid lightcurve inversion. II. The complete inverse problem." *Icarus* **153**, 37-51.

Neugent, K.F.; Slivan, S.M. (2008). "Rotation Periods and *H* Magnitudes of Two Koronis Family Members." *Minor Planet Bull.* **35**, 116-118.

Slivan, S.M. (2012). "Epoch Data in Sidereal Period Determination. I. Initial Constraint from Closest Epochs." *Minor Planet Bull.* **39**, 204-206.

Slivan, S.M. (2013). "Epoch Data in Sidereal Period Determination. II. Combining Epochs from Different Apparitions." *Minor Planet Bull.* **40**, 45-48.

Slivan, S.M. (2014). "Sidereal Photometric Astrometry as Efficient Initial Search for Spin Vector." *Minor Planet Bull.* **41**, 282-284.

Slivan, S.M. (2021). "Lightcurves, Sidereal Rotation Period, Spin Pole, and Convex Model Shape of Koronis Family Asteroid (1443) Ruppina." *Minor Planet Bull.* **48**, 331-334.

Stephens, R.D. (2018). "Asteroids Observed from CS3: 2017 July-September." *Minor Planet Bull.* **45**, 50-54.

Stephens, R.D.; Warner, B.D. (2020). "Main-Belt Asteroids Observed from CS3: 2020 April to June." *Minor Planet Bull.* **47**, 275-284.

Tonry, J.L.; Denneau, L.; Heinze, A.N.; Stalder, B.; Smith, K.W.; Smartt, S.J.; Stubbs, C.W.; Weiland, H.J.; Rest, A. (2018). "ATLAS: A High-cadence All-sky Survey System." *PASP* **130**, 064505.